Supplemental Information

A Size Barrier Limits Protein Diffusion

at the Cell Surface to Generate

Lipid-Rich Myelin-Membrane Sheets

Shweta Aggarwal, Larisa Yurlova, Nicolas Snaidero, Christina Reetz, Steffen Frey, Johannes Zimmermann, Gesa Pähler, Andreas Janshoff, Jens Friedrichs, Daniel J. Müller, Cornelia Goebel, and Mikael Simons

Inventory of Supplementary Material:

1. Supplemental Figures
   1. **Figure S1**
   2. **Figure S2**
   3. **Figure S3**
   4. **Figure S4**
   5. **Figure S5**

2. Supplemental Figure legends
Figure S1 (related to Figure 1).
Characterization of the cellular system to analyze biogenesis of myelin-membrane sheets.
Figure S2 (related to Figure 3).
F-actin and microtubule depolymerisation does not lead to a redistribution of CNPase to myelin-membrane sheets
Figure S3 (related to Figure 4).
Replacing the cytoplasmic domain of MAG or Tmem10/Opalin with a series of either positively or negatively charged amino acids does not influence their distribution.
Figure S4 (related to Figure 5).
 Immunogold labelling by the GFP antibodies in wild-type mouse to reveal backround staining of the antibody
Figure S5 (related to Figure 6).
Characterization of the biomimetic membrane system employed to reconstitute barrier properties of MBP _in vitro._

3. Supplemental Experimental Procedures
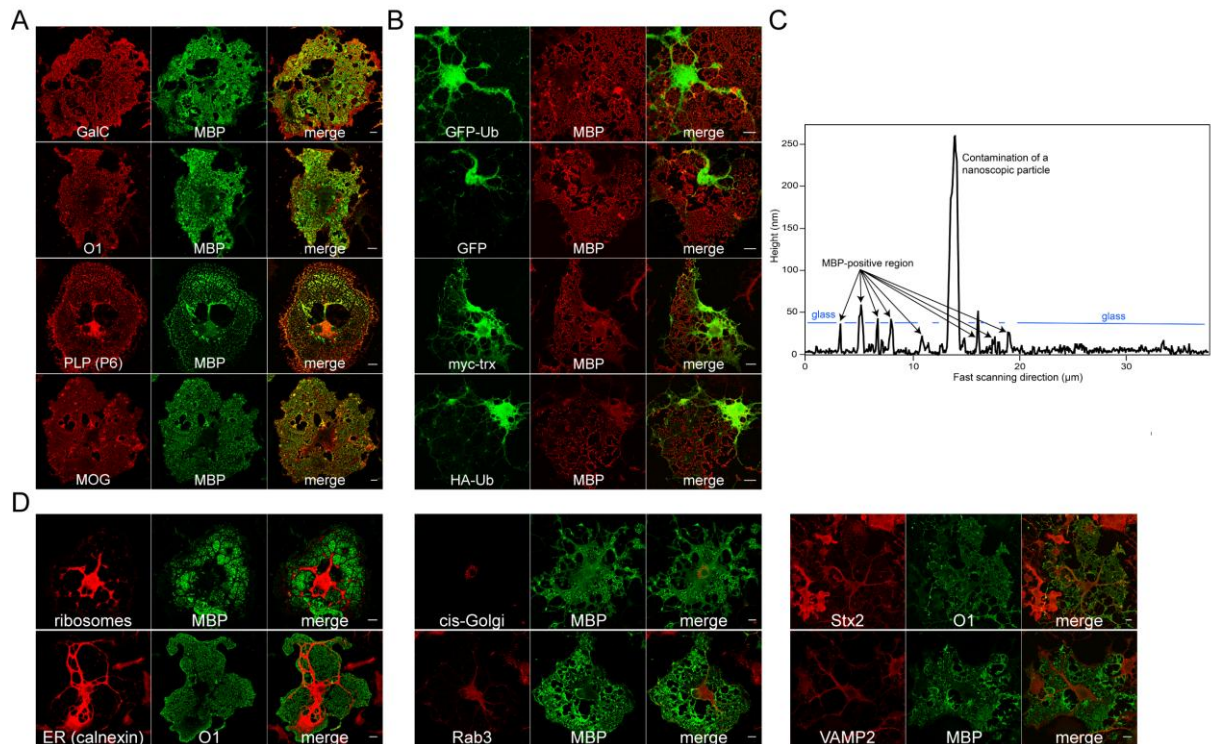
4. Supplemental References

Fig. S1

Figure S1 (referring to Figure 1). Characterization of the cellular system to analyze biogenesis of myelin-membrane sheets.

(A) Galactosylceramide, PLP and MOG localize to myelin-membrane sheets. Oligodendrocytes were immunostained for galactosylceramide (with GalC and O1 antibodies), PLP (with P6 antibody) and MOG. Membrane sheets were visualized by co-immunostaining for MBP. Scale bar, 10 µm.

(B) Cytosolic proteins with decreasing Stoke's radius are restricted from diffusing into myelin-membrane sheets. GFP, Myc-thioredoxin (Myc-trx) and HA-Ubiquitin (HA-Ub) were expressed in oligodendrocytes for 16 h and then co-stained for MBP. Myc-thioredoxin and HA-Ubiquitin were visualized by staining with Myc and HA antibodies, respectively. Scale bar, 10 µm.

(C) Representative AFM height profile of MBP positive regions is shown. The MBP positive regions were identified with the help of fluorescence microscopy. To record the AFM height profile, the AFM cantilever was manually positioned to cover MBP-positive regions. Then a 40 µm long height profile of the MBP-positive regions laying on the glass support was recorded. MBP-positive regions are indicated by arrows and areas showing the bare glass support by blue lines. The MBP-positive regions extend laterally over ≈2-3 µm and show heights varying between 20 and 50 nm. The large peak in the middle of the height profile results from a contaminating nanoscopic particle.

(D) Oligodendrocytes were immunostained for the ripbosomal protein - PS6, calnexin, the cis-Golgi marker - GM130, Rab3, Syntaxin2 (Stx2), and VAMP2 to visualize the ribosomes, the ER, the cis-Golgi and components of the fusion machinery, respectively. MBP was used as a marker for the membrane sheets. Scale bar, 10 µm.
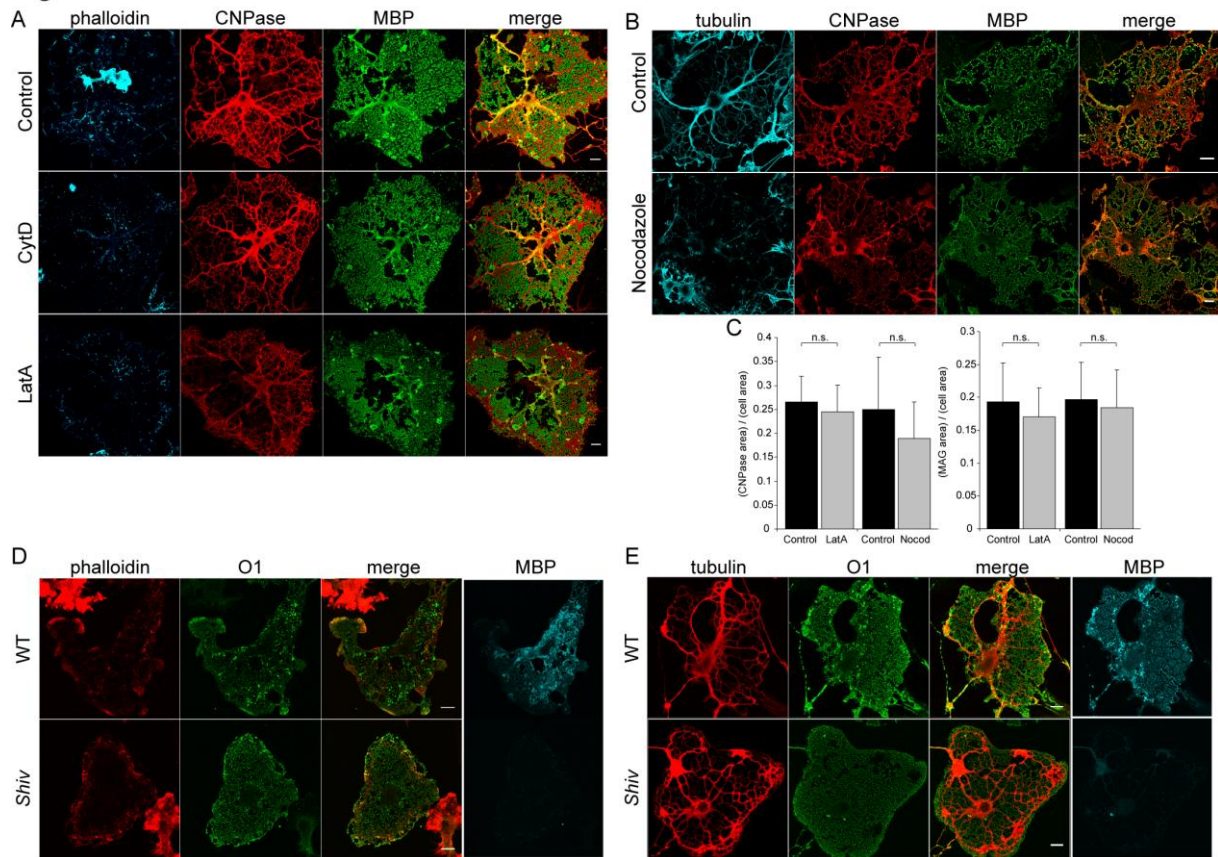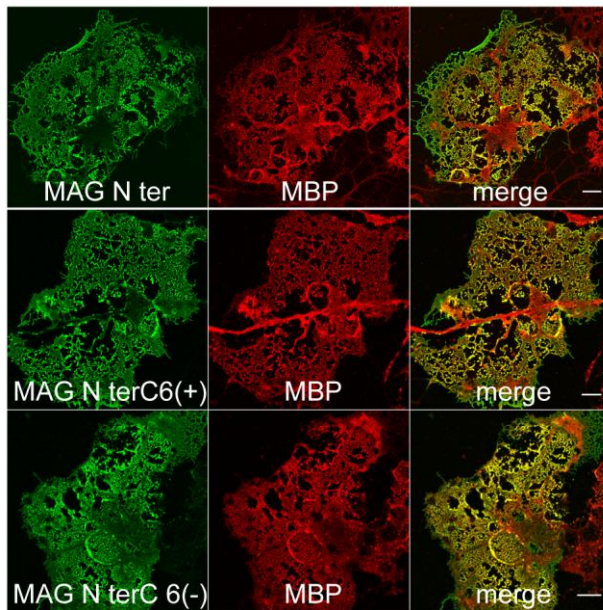
Fig. S2

Figure S2 (referring to Figure 3). Distribution of CNPase is unaffected upon F-actin and microtubule depolymerisation. (A) Oligodendrocytes were incubated with cytochalasin D (CytD; 2 µM, 2 h) or latrunculin A (LatA; 5 µM, 2 h) to induce actin depolymerisation and later immunostained for CNPase and MBP. F-actin was visualized with rhodamine-labelled phalloidin. (B) Oligodendrocytes were incubated with nocodazole (Nocod.; 2.5 µg/mL, 2 h) to induce microtubular depolymerisation and immunostained for CNPase and MBP. Microtubules were labeled with antibodies against tubulin. Scale bar, 10 µm. (C) Quantification of relative cell area occupied by indicated proteins in control, latrunculin and nocodazole treated cells. Bars show mean ± s.d. (n=~20, p>0.05, n.s. indicates no significant difference).

(D) In MBP deficient oligodendrocytes, F-actin, microtubules are not redistributed into the membrane sheets. Oligodendrocytes were prepared form mice lacking functional MBP (*shiverer*) and cells were immunostained for galactosylceramide (O1) to visualize membrane sheets and for MBP to show its absence in oligodendrocytes from *shiverer* mice. (D) F-actin was visualized with rhodamine-labelled phalloidin (E) and microtubules by immunostaining with antibodies against tubulin. Scale bar, 10 µm.
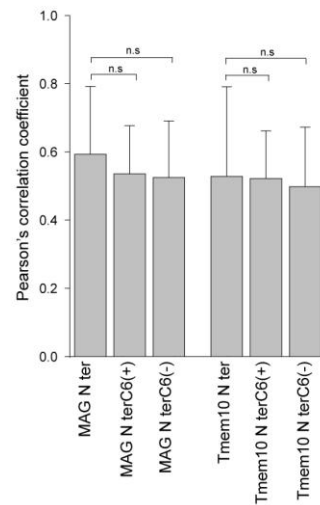
Fig. S3

Figure S3 (referring to Figure 4). Replacing the cytoplasmic domain of MAG or Tmem10/Opalin with a series of either positively or negatively charged amino acids does not influence their distribution. The cytoplasmic domain of MAG and Tmem10/Opalin were deleted and replaced by four glycines followed by either 6 positively or negatively charged amino acids. (A) Mutant forms of MAG that were expressed in oligodendrocytes, stained for the extracellular myc-tag and myelin-membrane sheets were visualized by co-immunostaining for MBP. Scale bar, 10 µm. (B) Quantification showing colocalization of the indicated proteins with MBP. Bars show mean ± s.d. (n=~40, p>0.05, ANOVA, n.s. indicates no significant difference). Charge did not influence the distribution of MAG or Tmem10 into myelin-membrane sheets. Please note that all charged forms of MAG and Tmem10/Opalin have only ~10 amino acids within the cytoplasmic domain.

Fig. S4

Figure S4 (referring to Figure 5). Immunogold labelling by the GFP antibodies in wild-type mouse to reveal backround staining of the antibody. (A) Optic nerve from wild-type (WT) mice (6 months old) was processed for immunoelectron microscopy and immunostained with the GFP antibody. Only very small amount of GFP labelling was found in the wild-type mice. Scale bar, 200 nm. (B) Quantification for % of total labelling shows that background staining occurred mainly in compact myelin. The staining observed in the inner tongue of 13aaPLP-GFP transgenic mice (presented in Fig. 5A) is therefore specific. Bars show mean ± s.d. (n=3 animals)

Fig. S5

A 1. SLB 2. GUVs

DHPE-Texas Red

B 1. SLB 2. MBP 3. Non labeled- GUVs 4. R3-GFP

R3-GFP   DHPE-Texas Red

C recombinant MBP (µg)

0.5   1.0   2.0   4.0   250,000 cells each

D 1.GUVs 2. O4 ab

DHPE-Texas Red

E 1.SLB 2.O4 ab 3.R3-GFP 4.GUVs

R3-GFP   DHPE-Texas Red

F 1.SLB 2.MBP 3.R3-GFP 4.GUVs

R3-GFP   DHPE-Texas Red

G 1.SLB 2.MBP(5µg) 3.R3-GFP 4.GUVs

R3-GFP   DHPE-Texas Red

1.SLB 2.MBP(2µg) 3.R3-GFP 4.GUVs

R3-GFP   DHPE-Texas Red

1.SLB 2.MBP(0.2µg) 3.R3-GFP 4.GUVs

R3-GFP   DHPE-Texas Red

H 1.SLB 2.MBP 3.GUVs

DHPE-Texas Red   DHPE-Texas Red   DHPE-Texas Red

I R3-GFP

GUVs − + + + + + + +

250 kD
70 kD
55 kD
35 kD
27 kD

DFDNB DSG DMA DMP DMA DMS DSS

J MBP (14KD)

GUVs − + + + + + + +

250 kD
70 kD
55 kD
35 kD
27 kD
15 kD

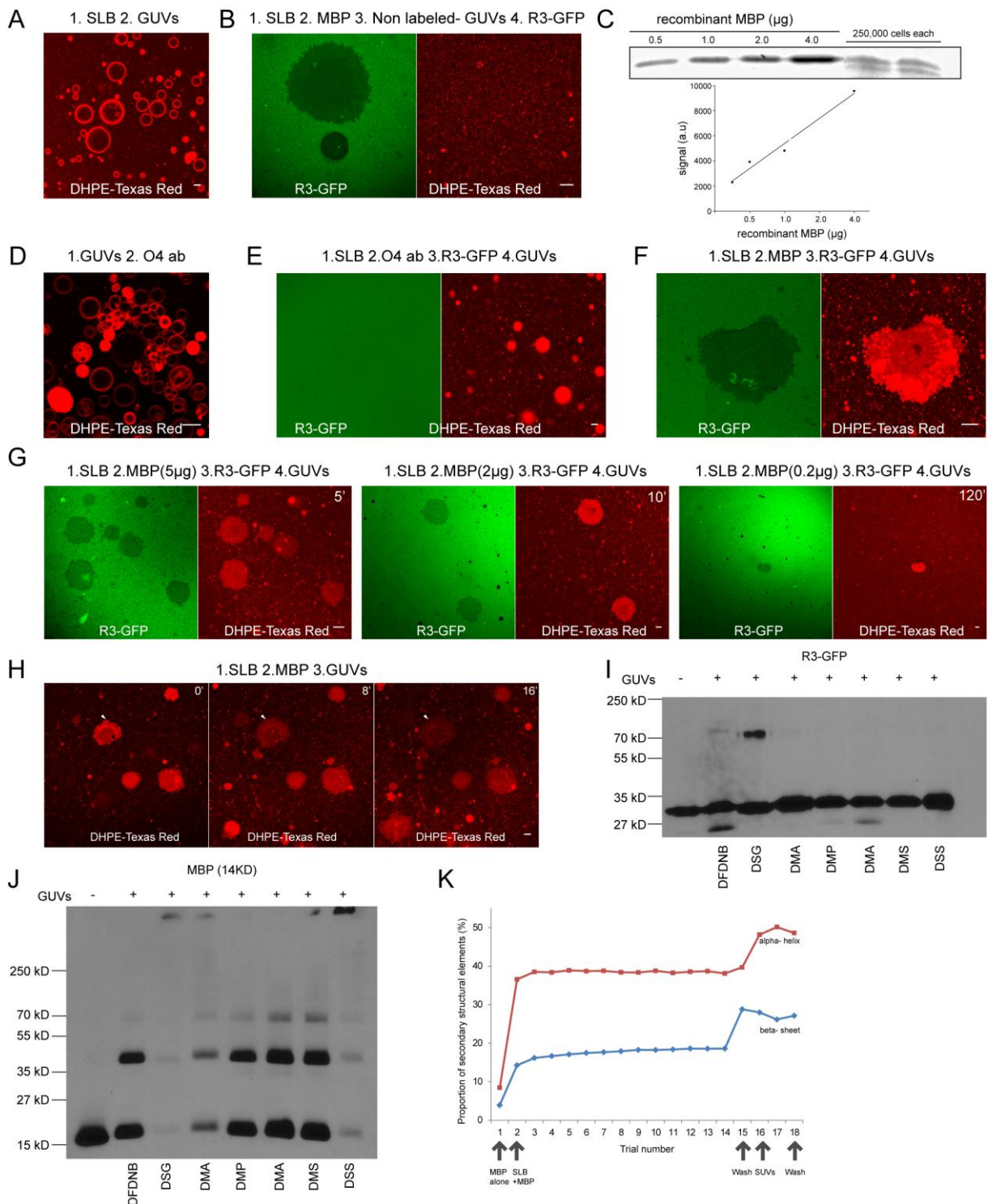DFDNB DSG DMA DMP DMA DMS DSS

K

Figure S5 (referring to Figure 6). Characterization of the biomimetic membrane system employed to reconstitute barrier properties of MBP *in vitro*.

(A) Control experiments using SLBs and GUVs as in Figure 6, but without any proteins added. SLBs were labelled with Cell Mask Orange and GUVs with 0.1mole% of DPPE-Texas Red. Scale bar, 10 µm.

(B) SLB experiments with non-labelled GUVs to control for quenching. Supported lipid bilayers (SLBs) mimicking inner leaflet myelin composition were prepared and visualized using 0.1mole% of DPPE-Texas Red. Purified 14 kDa MBP (7 µM) was

6

added to the SLB, followed by the addition of GUVs composed of PS: PC (1:2 mole %) and R3-GFP (7 µM). Scale bar, 10 µm.

(C) MBP amounts in a cell were estimated using primary oligodendroglial cell lysates (cultured for 7 days) together with MBP protein standards (for calibration), that were subjected to SDS-PAGE followed by coomassie staining. From the standard curve, we estimated ~$46*10^6 \pm 8*10^6$ (mean ± s.d.) MBP molecules per oligodendrocyte (n=4 independent experiments).

(D) Control experiments using O4 antibodies and GUVs composed of PC: PS: Sulfatide (2:1:1 mole%, visualized using 0.1mole% of DPPE-Texas Red). Addition of O4 antibodies (~10µg/ml) induced the aggregation of the GUVs. Scale bar, 10 µm

(E) Supported lipid bilayers (SLBs) using following lipid composition were prepared: 44% cholesterol, 15% 1,2-dioleoyl-*sn*-glycero-3-phosphoethanolamine (PE), 2% porcine brain L-α-phosphatidylinositol-4,5-bisphosphate (PIP2), 11.5% egg L-α-phosphatidylcholine (PC), 12.5% porcine brain L-α-phosphatidylserine (PS), 3% sphingomyelin (SM), 12% Porcine brain sulfatide and 0.1% of 1,2-dihexadecanoyl-sn-glycero-3-phosphoethanolamine (DHPE)-Texas Red. O4 antibodies (~10µg) were added to the SLBs followed by the addition of GUVs composed of PC: PS: Sulfatide (2:1:1 mole%, visualized using 0.1mole% of DPPE-Texas Red). Even after repeated washing steps GUVs remained bound to the SLBs. However, no extrusion of R3-GFP was observed. Scale bar, 10 µm

(F) When control experiments were performed with MBP and the GUVs and SLBs with the lipid composition as in E, spreading of the GUVs and extrusion of the R3-GFP was observed. Scale bar, 10 µm

(G) Experiments performed as described in Fig. 6A using different concentration of MBP. First, purified recombinant R3-GFP (7 µM) was added onto the SLBs, followed by the addition of purified recombinant 14 kDa MBP in different concentration (indicated in the image) and GUVs composed of PS and PC in 1:2 molar ratios (0.1mole% of DHPE-Texas Red was used to visualize the GUVs). The time required to induce the spreading of the GUVs and the extrusion of the R3-GFP is indicated on the upper right side of each image (in min). Similar results were observed when MBP was added at lower concentration, except that more time was required before spreading and extrusion was observed. Scale bar, 10 µm.

(H) Signal intensities of DHPE-Texas Red decrease with time in the GUVs (PS and PC in 1:2 molar ratios; 0.1mole% of DHPE-Texas Red). Time in minutes is shown on the upper right side of each image. Scale bar, 10 µm.

(J) Chemical cross-linking experiments between MBP and GUVs: 200 ng MBP was added to a solution of GUVs (PC:PS- 2:1 mole%) and incubated for 30 min at room temperature, followed by the addition of indicated cross-linkers at a final concentration of 30 µM. The cross-linking experiment was performed for 30 min followed by quenching using 1M glycine at a final concentration of 50 mM. (I) Control experiments were performed in a similar way using 200ng of R3-GFP.

(K) Attenuated total reflection Fourier transform infrared spectroscopy (ATR-FTIR) of MBP. SUVs (V = 30 µL, c = 1 mg/mL) were added to the ATR FT IR crystal and the solution was heated to 50°C. SLBs were obtained by cooling the system to room temperature. This was followed by the addition of MBP (at a final concentration of 1.3 mg/mL in the measurement cell). After 30 min incubation, samples were rinsed and 20 µL of SUV solution was added on top of the MBP bound SLBs, followed by rinsing to remove unbound vesicles. Trial 1: MBP in solution, Trial 2-14: MBP bound to SLBs, Trial 15: washing off the unbound MBP, Trial 16-17: SUV addition on top of MBP bound SLBs, Trial 18: washing off the unbound SUVs. Note the further change in secondary structure of MBP upon addition of SUVs (Trial 16-18).

Supplemental Experimental Procedures

Expression plasmids
MOG-GFP (generously provided by M. Ameloot, Hasselt University, Belgium), pmaxGFP (Lonza Group Ltd, Basel, Switzerland), pEGFP-N1, pDsRed2-C1 (Clontech, Mountain View, CA, USA), S- and L-MAG (a kind gift from N. Schaeren-Wiemers, University Hospital of Basel, Swizerland), Myc-trx (Liu et al., 2000) (D. Russell, UTSW, USA; Addgene, HA-Ub (Kamitani et al., 1997) (E. Yeh, University of California, USA; Addgene, Neurofascin-155 (a kind gift from E. Peles, Weizmann Institute, Israel). The following plasmids were constructed:

Plasmid name	Template	Species	bp (aa)	5'seq	3'seq
pcDNA3.1-S-MAG N ter	S-MAG	mouse	20-536	AAAAAAAAAAGCGCTGTGGGCGTGGGGGGCCACTGGG	TTTTTTTTTTAAGCTTTCACGTCTGGGTGATGTAGCACACAATG
pcDNA3.1- S- MAG N terC10	S-MAG	mouse	20-546	AAAAAAAAAAGCGCTGTGGGCGTGGGGGGCCACTGGG	TTTTTTTTTTAAGCTTTCAGGAGCTCTCCGTGAC
pcDNA3.1-S-MAG N terC20	S-MAG	mouse	20-556	AAAAAAAAAAGCGCTGTGGGCGTGGGGGGCCACTGGG	TTTTTTTTTTAAGCTTTCAGACATGAGGGTTGTCTCC
pcDNA3.1-S-MAG N terC30	S-MAG	mouse	20-566	AAAAAAAAAAGCGCTGTGGGCGTGGGGGGCCACTGGG	TTTTTTTTTTAAGCTTTCACCCAGAGATTCTGAATTCGG
pcDNA3.1-S-MAG N terC36	S-MAG	mouse	20-572	AAAAAAAAAAGCGCTGTGGGCGTGGGGGGCCACTGGG	TTTTTTTTTTAAGCTTTCACTCATACTTATCAGGTGCCC
pcDNA3.1-Tmem10N ter	Tmem10	human	1-57	AAAAAAAAAAGCGCTATGAGTTTTTCACTGAACTTCAC	TTTTTTTTTTAAGCTTTCATCTTCTTCGGTGAATCAAAGTAAATAG
pcDNA3.1-Tmem10N terC10	Tmem10	human	1-63	AAAAAAAAAAGCGCTATGAGTTTTTCACTGAACTTCAC	TTTTTTTTTTAAGCTTTCACATGGCCTCAATGCTG
pcDNA3.1-Tmem10N terC20	Tmem10	human	1-73	AAAAAAAAAAGCGCTATGAGTTTTTCACTGAACTTCAC	TTTTTTTTTTAAGCTTTCATGAAATTTCACATGGTCTGTC
pcDNA3.1-Tmem10N terC30	Tmem10	human	1-83	AAAAAAAAAAGCGCTATGAGTTTTTCACTGAACTTCAC	TTTTTTTTTTAAGCTTTCACTCAGATATCTTGGGATTGTC
pcDNA3.1-Tmem10N terC40	Tmem10	human	1-93	AAAAAAAAAAGCGCTATGAGTTTTTCACTGAACTTCAC	TTTTTTTTTTAAGCTTTCACTTCTCATGTGTGGGTGATC
pcDNA3.1-Tmem10N ter(HA)	Tmem10	human	1-57	AAAAAAAAAAGCGCTATGAGTTTTTCACTGAACTTCAC	TTTAAGCTTTCACTCGAGAGCGTAATCTGGAACATCGTATGGGTATCCTCCTCCTCTTCTTCGGTGAATCAAAG
pcDNA3.1-Tmem10N terC20(HA)	Tmem10	human	1-73	AAAAAAAAAAGCGCTATGAGTTTTTCACTGAACTTCAC	TTTAAGCTTTCACTCGAGAGCGTAATCTGGAACATCGTATGGGTATCCTCCTCCCATGGCCTCAATGCTG
pcDNA3.1-Nfas155	Neurofascin155	rat	25-1189	AAAAAAAAAAGCGCTATGGCCAGGCAGCAG	TTTTTTTTTTAAGCTTTCAGGCCAGGGAATAGATG
pcDNA3.1-Nafs155 N ter	Neurofascin155	rat	25-1132	AAAAAAAAAAGCGCTATGGCCAGGCAGCAG	TTTTTTTTTTAAGCTTTCACTTGATGAAGCAGACGATCAG
pcDNA3.1-Nafs155 N terC30	Neurofascin155	rat	25-1109	AAAAAAAAAAGCGCTATGGCCAGG	TTTTTTTTTTAAGCTTTCATGAACCATCTTCTTCTTTGGG
pcDNA3.1- S- MAG N terC6(+)	S-MAG	mouse	20-536	AAAAAAAAAAGCGCTGTGGGCGTGGGGGGCCACTGGG	TTTTTTTTTTAAGCTTTCAGTCGTCGTCGTCGTCTCCTCCTCCTCCCGTCTGGGTGATGTAGC
pcDNA3.1- S- MAG N terC6(-)	S-MAG	mouse	20-536	AAAAAAAAAAGCGCTGTGGGCGTGGGGGGCCACTGGG	TTTTTTTTTTAAGCTTTCATCTTCTTCTTCTTCTTCCTCCTCCTCCCGTCTGGGTGATGTAGC
pcDNA3.1-Tmem10N terC6(+)	Tmem10	human	1-57	AAAAAAAAAAGCGCTATGAGTTTTTCACTGAACTTCAC	TTTTTTTTTTAAGCTTTCATCTTCTTCTTCTTCTTCCTCCTCCTCCTCTTCTTCGGTGAATCAAAG

pcDNA3.1-Tmem10N terC6(-)	Tmem10	human	1-57	AAAAAAAAAAGCGCTAT GAGTTTTTCACTGAACTT CAC	TTTTTTTTTAAGCTTTCAGTC GTCGTCGTCGTCGTCTCCTC CTCCTCCTCTTCTTCGGTGAA TCAAAG

The GFP-MOG construct was generated by insertion of the pHluorin sequence (G. Miesenboeck, University of Oxford, UK) into the MOG full-length construct after the MOG signal sequence. Myc-thrombin-HA-MOG reporter construct was generated by fusing myc (E Q K L I S E E D L) and HA (Y P Y D V P D Y A) tags separated by a thrombin cleavage sequence (L V P R G S) to the N-terminus of MOG after the signal sequence of MOG. CD9-eGFP and CD81-eGFP were constructed by sub-cloning CD9 and CD81 cDNA into pEGFP-N1 vector (clonetech) between HindIII and XhoI sites in the multiple cloning regions. Mem-YFP contains the lipid-anchored N-terminal 20 amino acids of GAP43.

E. coli expression vectors

Plasmids allowed for recombinant expression of indicated proteins in *E. coli*. Complete plasmid sequences are available on request (Table S1).

Table S1: E.coli expression vectors.[a]

Name	expressed protein
pSF1622	H14-MalE-SUMO-NHE3_R1-GFP
pSF1623	H14-MalE-SUMO-NHE3_R2-GFP
pSF1624	H14-MalE-SUMO-NHE3_R3-GFP
pSF1625	H14-TEV-MBP14-Cys

[a] Abbreviations: His$_{14}$, histidine tag; MalE: *E.coli* maltose-binding protein; NHE3_R1/R2/R3, (Alexander et al. 2011) ; MBP, myelin basic protein.

ATR (attenuated total reflection) and transmission FT IR spectroscopy

Protein used for IR measurements were 5x lyophilized from 0.05 M HCl to replace trifluoroacetate counterions at protein backbone against chloride ions (Andrushchenko et al., 2007). All experiments were carried out in D_2O containing 120 mM KCl at a Vertex 70 FTIR (Bruker Optics, Ettlingen, Germany). Spectra were acquired using a MCT detector and a resolution of 2 cm^{-1}. All spectra were corrected for water vapour and CO_2 vibrations. Pure MBP was measured in solution (c_{MBP} = 4 mg/mL, M_{MBP} = 18 kDa) using a transmission FTIR cell for liquids (AquaSpec, Bruker Optics, Ettlingen, Germany). To monitor the binding of MBP to lipids, a solid supported lipid bilayer (SSLB) was spread on a ZnSe crystal covered with Si mounted to an ATR-FTIR measurement cell (BioATRII, Bruker Optics, Ettlingen, Germany). Therefore, lipid stock solutions in chloroform (c_{lipid} = 1-10 mg/mL) were mixed in a test tube and chloroform was removed to produce a lipid film with the desired composition. These films were then dissolved in D_2O containing 120 mM KCl at a concentration of 1 mg/mL, to obtain multilamellar vesicles which can be transformed into single unilamellar vesicles (SUV; containing 80% PC, 18% PS, 2% PIP2; 1 mg/mL) by sonication (50 W, 0.4 s Puls, 30 min) in a vessel resonator (Sonoplus HD 2070, Bandelin, Berlin, Germany). Solid supported lipid bilayers (SSLB) were formed by spreading SUV on the Si surface of the ZnSe crystal at temperatures above phase transition temperature T_m of used lipids (Reimhult et al., 2002). Secondary structure analyses were carried out using QUANT2 software package provided in the OPUS 6.5 software (Bruker Optics, Ettlingen, Germany).

This software provides a library of 43 different proteins and compares it with the measured data to determine the percentage of secondary structure of sample.

Supplemental References

Alexander, R. T., Jaumouille, V., Yeung, T., Furuya, W., Peltekova, I., Boucher, A., Zasloff, M., Orlowski, J., and Grinstein, S. (2011) Membrane surface charge dictates the structure and function of the epithelial Na+/H+ exchanger. Embo J *30*, 679-691.

Andrushchenko, V. V., Vogel, H. J., and Prenner, E. J. (2007). Optimization of the hydrochloric acid concentration used for trifluoroacetate removal from synthetic peptides. J Pept Sci *13*, 37-43.

Liu, H., Nishitoh, H., Ichijo, H., and Kyriakis, J. M. (2000). Activation of apoptosis signal-regulating kinase 1 (ASK1) by tumor necrosis factor receptor-associated factor 2 requires prior dissociation of the ASK1 inhibitor thioredoxin. Mol Cell Biol *20*, 2198-2208.

Kamitani, T., Kito, K., Nguyen, H. P., and Yeh, E. T. (1997). Characterization of NEDD8, a developmentally down-regulated ubiquitin-like protein. J Biol Chem *272*, 28557-28562.

Reimhult, E., Hook, F., and Kasemo, B. (2002). Temperature dependence of formation of a supported phospholipid bilayer from vesicles on SiO2. Phys Rev E Stat Nonlin Soft Matter Phys *66*, 051905.